Radiative transfer for IASI

Marco Matricardi

ECMWF, Shinfield Park, Reading, Berkshire, RG2 9AX, UK
marco.matricardi@ecmwf.int

Abstract

IASI measurements of spectral radiances made between the 1st April 2008 and the 15th April 2008 are compared with simulations performed using the RTTOV fast radiative transfer model utilizing regression coefficients based on different line-by-line models. The comparisons are performed within the framework of the European Centre for Medium-Range Weather Forecasts Integrated Forecasting System using fields of temperature, water vapour and ozone obtained from short-range forecasts. Simulations are performed to assess the accuracy of the RTTOV computations and investigate relative differences between the line-by-line models and the quality of the spectroscopic databases on which the RTTOV coefficients are based.

1. Introduction

The exploitation of satellite radiance data for Numerical Weather Prediction (NWP) requires the use of an accurate and fast radiative transfer (RT) model to simulate radiances from an input atmospheric profile. The low noise level of IASI makes RT errors an important contribution to the definition of the observation-error covariance matrix and consequently RT errors must be properly evaluated and their origin fully understood.

Fast RT model errors are dominated by two main components: the parameterization used for the atmospheric transmittances and the errors associated with the spectroscopic parameters and the computational procedures adopted in the line-by-line (LBL) models on which fast RT models are generally based. The fast RT model used operationally at the European Centre for Medium-Range Weather Forecasts (ECMWF) is the Radiative Transfer Model for TOVS (RTTOV) (Saunders et al. 1999). Errors associated to the RTTOV transmittance parameterization for the IASI channels are discussed in detail in Matricardi (2008) whereas LBL model errors have been investigated in several studies (e.g. Rizzi et al. 2002; Tjemkes et al 2003) using high-spectral resolution aircraft data.

In this paper we try to assess the absolute accuracy of the RTTOV model as a whole. The availability of RTTOV regression coefficients based on different LBL models has also offered the opportunity to investigate relative differences between LBL-models and the quality of the spectroscopic databases used in the LBL-model computations. The assessment of the RTTOV accuracy has been carried out by running a number of Integrated Forecast System (IFS) monitoring experiments where IASI spectra simulated by RTTOV have been compared to IASI spectra measured during the period 1st April 2008-15th April 2008 using short range operational forecasts of temperature, water vapour and ozone fields to specify the RTTOV input state vector.

2. The monitoring experiments

Three baseline monitoring experiments have been run using cycle 33R1 of the IFS (which was the operational cycle from June until October 2008) using the T799 horizontal truncation. This truncation corresponds to a horizontal resolution of ~25 km. A feature of cycle 33R1 of the IFS is a vertical discretization of the atmosphere into a grid of 91 pressure levels. The model uses a hybrid vertical coordinate with coordinates that follow the horography of the terrain in the lower troposphere and pressure coordinates

in the stratosphere above about 60 hPa. The top level is fixed at 0.01 hPa (about 80 km) and of the 91 levels in the vertical, 52 are above 100 hPa. The state vector variables used in the RTTOV simulations are forecast fields of temperature, humidity, ozone and surface parameters. IASI data within a 12-hour 4D-VAR window are grouped into 30 minutes time slots. A T799 high resolution forecast is then run from the previous analysis and observation minus model differences are computed for IASI soundings within a given time slot. This sequence is then repeated for each 12-hour 4D-VAR window. In this study we consider IASI data inside 12-hour 4D-VAR windows during the period 1st April 2008-15th April 2008.

The IASI spectra used in our experiments are measured over the sea. Only channels detected as clear by the ECMWF cloud detection algorithm are processed. Since the ECMWF cloud detection algorithm (McNally and Watts 2003) finds clear channels rather than clear locations, the size of sample varies with the sensitivity of the channel to clouds. This is illustrated in Fig. 1 where it can be seen that the size of the sample varies from several thousands spectra for the channels peaking at middle and high altitudes to a few thousands for channels peaking at low altitudes or at surface. To avoid reflected solar radiation and non-LTE effects (the latter are not modelled in RTTOV), in the spectral region between 2000 and 2760 cm^{-1} we have sampled only night-time spectra. Consequently, the size of the sample in this spectral region is significantly smaller than the size of the sample in other spectral regions.

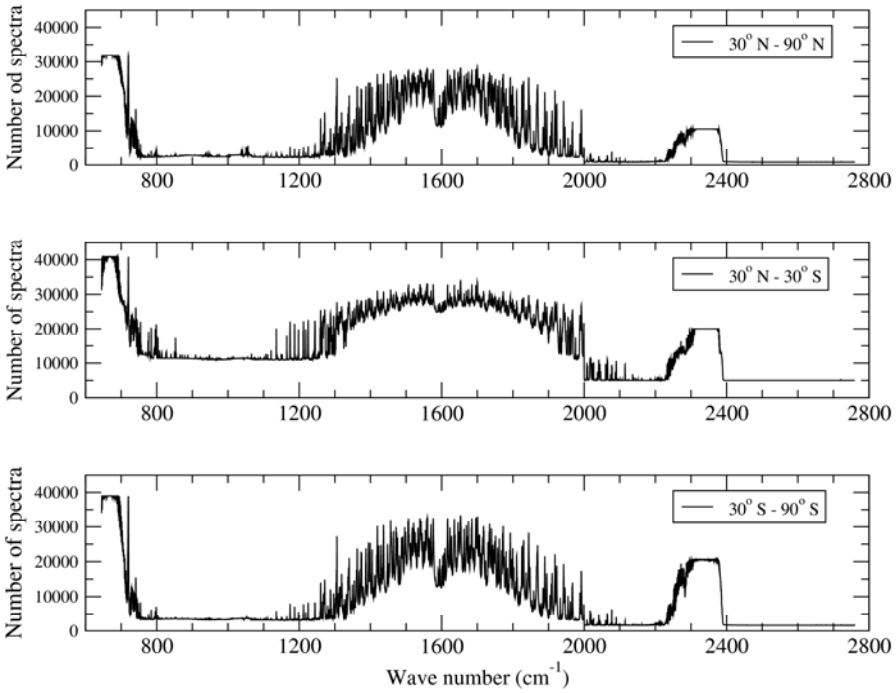

Figure 1: The number of spectra sampled as clear for each IASI channel for three different latitude bands.

2.1. The line-by-line models

RTTOV regression coefficients for IASI are available based on various LBL models. Regression coefficients based on version 4 of the GENLN2 LBL model (GENLN2_v4) and version 11.1 of the LBLRTM LBL model (LBLRTM_v11.1) have been generated at ECMWF using RTTOV-9 predictors (Matricardi, 2003) whereas coefficients based on version 1.11 of the kCARTA LBL model (kCARTA_v1.11) have been generated at Meteo France using RTTOV_8 predictors (Matricardi et al., 2004). A brief description of the LBL models is given in the following sections.

2.1.1. GENLN2_v4

GENLN2_v4 (Edwards 1992) is a line-by-line atmospheric transmittance and radiance model. The GENLN2_v4 CO_2 line shape includes the effect of line mixing and takes into account the sub-Lorentzian behaviour in the far-wing of the line. If data is available, CO_2 Q-branch line mixing in the *υ2* and *υ3* band can be included out to an arbitrary 10 cm^{-1} from line centre. For greater distances from the centre the line shape is approximated by the empirical model by Cousin et al. (1985). This model explains the sub-Lorentzian nature of the CO_2 far wing line shape in terms of duration of collision effects and uses a temperature dependent χ-factor to adjust the standard line shape function based on the impact theory. If no line-mixing data is available then the sub-Lorentzian line shape is used everywhere. The standard release of GENLN2_v4 includes the water vapor continuum model CKD_2.1. However, we carried out our computations using the model CKD_2.4 (Clough et al. 1989) that became available at the time the regression coefficients were about to be generated. In our computations, CO_2 Q-branch line mixing has been fully accounted for using first order line-mixing coefficients from Strow et al. (1994).

2.1.2. kCARTA_v1.11

The kCARTA_v11.1 model (De Souza-Machado et al., 2002) is a fast LBL algorithm where transmittances are computed from compressed look-up tables of atmospheric transmittances (Strow et al., 1998). The water vapour continuum model (hence after referred to as MTK_CKD_UMBC) is based on the MTK_CKD_2.0 (Tobin et. al. 1999) model. It uses revised values of the spectral density function coefficients based on measurements of AIRS spectra utilizing in-situ data available from the ARM sites (Machado, 2008). Line mixing coefficients for CO_2 are available for 12 P/R-branch bands and 12 Q-branch bands in the short wave and in the long wave. The kCARTA model for the CO_2 line shape is based on the work by Tobin (1996) and De Souza-Machado et al. (1999). For the P/R-branch it involves an approximation for the combination of line mixing and duration-of-collision effects. Regarding the UMBC-LBL model it should be stressed that it relies on a full treatment of the CO_2 Q- and P/R-branch line mixing and does not use the perturbation theory.

2.1.3. LBLRTM_v11.1

The LBLRTM line-by-line model (Clough et al., 1992) has been developed at the Atmospheric and Environmental Research Inc. (AER). LBLRTM incorporates the self- and foreign-broadened water vapor continuum model MT_CKD_2.0 (Tobin et. al. 1999). In LBLRTM the CO_2 line shape includes the effects of line mixing for the P-R-branch and Q-branch in the υ2 and υ3 band using first order line coupling parameters generated using the code by Niro et al. 2005. Since the model by Niro et al. (2005) combines the effects of line mixing and duration of collision effects, the χ factor is set equal to 1. In addition, the CO_2 continuum is computed using the Niro et al. (2005) coupling coefficients with a scaling factor of 0.75 applied to the ν3-band to agree with AIRS spectra in the ν3 spectral region.

The computation of the LBL transmittances is performed on a grid of vertical levels of fixed pressure for a regression dataset of diverse atmospheric profiles and require the use of appropriate parameters from a molecular database. These details are summarized in Table 1. Note how for kCARTA and GENLN2 the same molecular database has been used although it should be noted that for GENLN2 the use of the Strow et al.(1994) line mixing coefficients requires the use of CO_2 molecular line parameters from the HITRAN_1992 compilation. Based on the results shown in Matricardi (2007), for the LBLRTM computations we have envisaged a molecular database that blends line parameters obtained from various sources. This blended database is largely drawn from HITRAN_2004 (Rothman et al., 2005) and includes updates up to 1/1/2007. However, in the 9.8 micron ozone band we use ozone line parameters from HITRAN_2000 (Rothman et al., 2003) whereas in the spectral region between 1700 and 2400 cm^{-1} we use water vapour line parameters from GEISA_2003 (Husson et al., 2005). Note that the use of Niro et al. (2005) line mixing coefficients requires

that LBLRTM line parameters for CO_2 are obtained from the HITRAN_2000 compilation. From Table 1 it can also be seen that regression coefficients are based on different profile training sets and that all the computations have been performed on the 101 level vertical grid specified by the AIRS science team (Strow et al., 2003).

Table 1: The regression coefficients used for the RTTOV simulations

Coefficients	Continuum	CO2 line mixing	Molecular Database
LBL model: kCARTA Number of levels: 101 Profile training set: ECMWF_52_P	MTK_CKD_v2.0_UMBC	P/Q/R branch (υ2 and υ3 band)	HITRAN_2000
LBL model: GENLN Number of levels: 101 Profile training set: ECMWF_43_P	CKD_v2.4	Q branch (υ2 and υ3 band)	HITRAN_2000
LBL model: LBLRTM Number of levels: 101 Profile training set: ECMWF_83_P	MTK_CKD_v2.0	P/Q/R branch (υ2 and υ3 band)	HITRAN_2000 HITRAN_2004/2006 GEISA_2003

All LBL datasets include N_2, O_2, HNO_3, OCS, CCl_4, CF_4, CCl_3F and CCl_2F_2 among the gases with fixed amount. Regression coefficients based on the GENLN2 and LBLRTM models allow the variation of CO_2, N_2O, CO, and CH_4 amounts whereas in kCARTA the amount of these gas species is fixed. The LBLRTM dataset includes an additional number of fixed gas species, i.e. NO_2, SO_2 and NO. In general, atmospheric constituent profiles for all gases are based on AFGL profiles scaled to reflect present-day concentrations. However, in the LBLRTM dataset we have used HNO_3 and NO profiles generated using the MOZART chemical transport model (Hauglustaine et al., 1998) whereas in the kCARTA dataset the concentrations of CO_2, N_2O, CO and CH_4 are based on the climatological profiles described in Matricardi (2003).

In our RTTOV computations the state vector includes profiles of temperature, water vapour and ozone, surface parameters (e.g. skin temperature and surface pressure) and a wave number dependent value of the sea surface emissivity that includes the dependence on the viewing geometry. In addition to the profiles of temperature, water vapour and ozone, the experiments that use RTTOV coefficients based on GENLN2 and LBLRTM also require input profiles of CO_2, CO, N_2O and CH_4. Since profiles for these trace gases are not prognostic variables in the ECMWF model we had to fix the amounts in the GENLN2 and LBLRTM experiments. To this end we have chosen the values assumed in the LBL computation used to train kCARTA. The rationale behind this choice is that at present kCARTA coefficients are used operationally at ECMWF for the assimilation of AIRS and IASI radiances and we want to use the kCARTA spectra as benchmark in our comparisons.

3. Discussion of the Results

3.1. IASI band 1 (645 to 1200 cm^{-1})

Results in IASI band 1 are plotted in Fig.2, Fig. 3 and Fig. 4 where we show the mean value of the difference (bias) between observed and simulated radiances in units of equivalent black body brightness temperature for the northern hemisphere (30º N-90º N), tropics (30º N-30º S) and southern hemisphere (30º S-90º S) respectively. In the top panel the LBLRTM spectrum (solid red line) is superimposed on the kCARTA spectrum (solid black line) whereas in the bottom panel the GENLN2 spectrum (solid red line) is

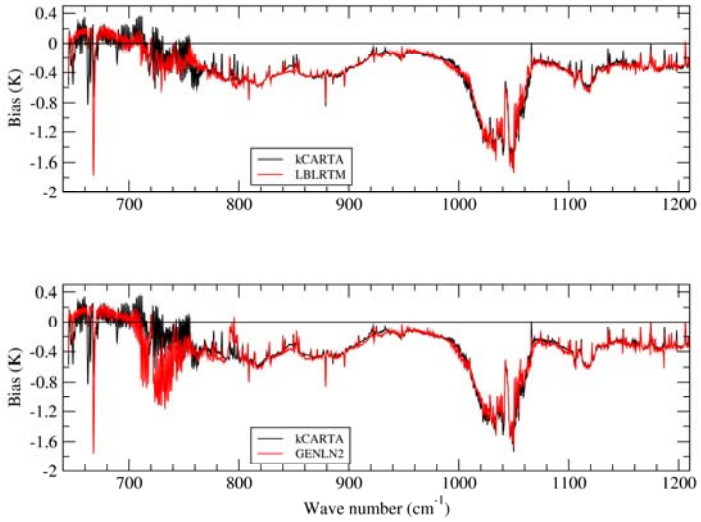

Figure 2: The mean value of the difference between observed and computed brightness temperatures in the northern hemisphere for IASI band 1.

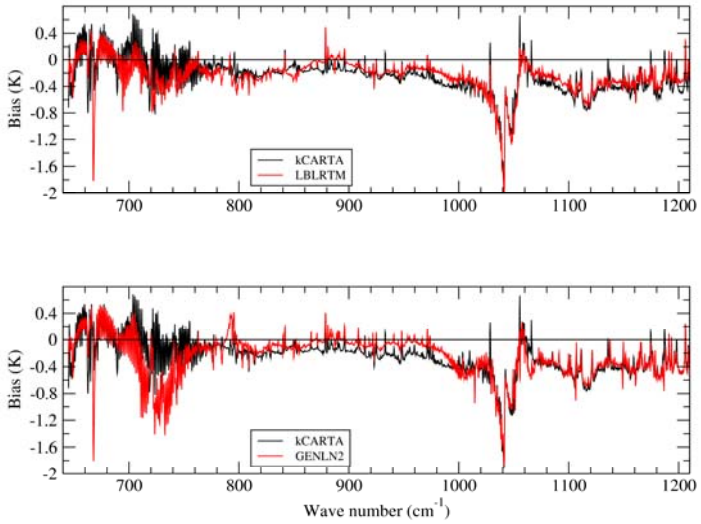

Figure 3: The mean value of the difference between observed and computed brightness temperatures in the tropical region for IASI band 1.

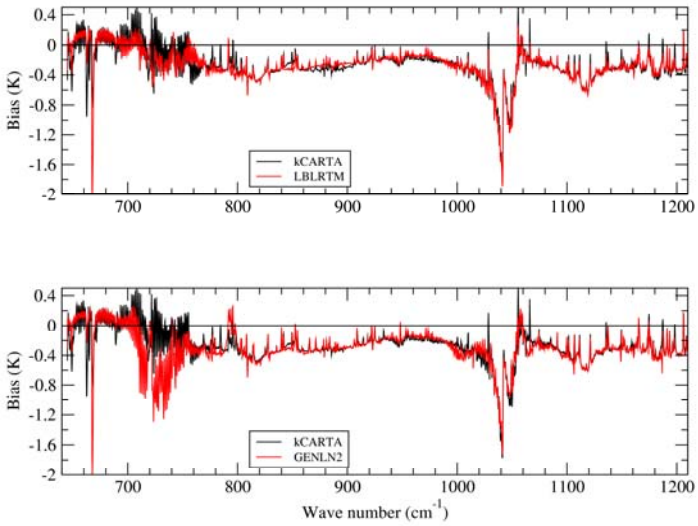

Figure 4: The mean value of the difference between observed and computed brightness temperatures in the southern hemisphere for IASI band 1.

superimposed on the kCARTA spectrum. Results show that for all experiments biases are generally within ±1K in all geographical regions. The only exception is the ozone band at 9.8 microns where biases can reach 1.5 K in the northern hemisphere.

3.1.1. Results in the temperature sounding band

Of particular interest are the result obtained in the 15 microns temperature sounding CO_2 ν2 band where the GENLN2 experiment shows significantly larger biases between 700 cm^{-1} and 750 cm^{-1}. We interpret this result in terms of errors in the GENLN2 CO_2 line shape due to the fact that the far-wing shape is computed using the Cousin et al. (1985) empirical model. As shown in Fig.4, Fig.5 and Fig.6, errors in the GENLN2 CO_2 line shape can significantly degrade the accuracy of the spectra.

In the same spectral region, kCARTA and LBLRTM biases are significantly smaller. The two models exhibit similar features with differences between the spectra smaller than 0.2K. However, the kCARTA spectrum is more irregular than the LBLRTM spectrum. This behaviour can be affected by factors that include the line mixing model, uncertainties in the temperature profile and errors in the strengths and widths of the weak water vapour lines originating from the edge of the water vapour pure rotational band. The errors in the line strengths and widths can either be due to uncertainties in the water vapour profile or due to spectroscopic errors (in addition to this kCARTA and LBLRTM use different water vapour molecular databases).

In the 645 to 700 cm^{-1} spectral region we note the very close similarities between the LBLRTM and GENLN2 spectra and the differences between these two models and kCARTA. These differences cannot be attributed to the molecular parameters since, for instance, LBLRTM and kCARTA use the same HITRAN_2000 compilation, and line mixing should not be significant in this region. Regarding the absolute value of the biases, it should be noted that in this spectral region a consistent number of channels is sensitive to emission at high altitudes and consequently biases can be affected by systematic temperature errors of the ECMWF model in the upper stratosphere and mesosphere.

A feature in common to the LBLRTM and GENLN2 spectra is the large bias (between 1.8K and 2K) seen in correspondence to the fundamental CO_2 Q-branch at 667 cm^{-1}. The origin of this bias is difficult to interpret. Masiello et al. (2009) suggest that, at least for LBLRTM, the large biases are the result of errors in the CO_2 continuum model. However, this does not explain the GENL2 behaviour. The fact that GENLN2 and LBLRTM use line mixing coefficients based on a 1st order perturbation theory could point to the fact that this approximation might not be adequate al least for those channels affected by line mixing.

3.1.2. Results in the ozone sounding band

Spectra in the ozone band are remarkably close. Biases observed in the ozone band are probably dominated by spectroscopic errors although the larger values (up to -1.6K) observed in the northern hemisphere might reflect a poor performance of the ozone assimilation system.

3.1.3. Results in the window regions

The absorption in the window regions between 800 and 1200 cm^{-1} consists mainly of the absorption due to water vapour self- continuum although in the high-wavenumber boundary of the window (i.e. between 1080 and 1200 cm^{-1}) the contribution of weak water vapour lines has also to be taken into account. With the exception of a few channels, the specification of the continuum model and the choice of the molecular parameters do not appear to have a significant impact on the spectra obtained in the northern and southern hemispheres. In fact, within each of these geographical regions, spectra are very similar with biases varying between -0.1 and -0.6 K in the northern hemisphere and between -0.1 and -0.4 K in the southern hemisphere.

Results for the tropical region (Fig. 3) show that in contrast to the cases discussed above, differences exist between the spectra in the window regions. In fact, the high tropical water vapour column concentrations

make the water vapour continuum absorption a much more important factor. We have studied this aspect more in depth by running a further experiment where the kCARTA spectra have been computed using the same water vapour continuum model used in the LBLRTM model. The results are shown Fig.5 where we have plotted the difference between the standard kCARTA mean spectrum and the LBLRTM mean spectrum (top panel) and the difference between the modified kCARTA mean spectrum and the LBLRTM mean spectrum (bottom panel).

Fig.5 shows that the use of the same continuum model greatly reduce the differences between the spectra.between 800 and 980 cm^{-1}. The residuals seen in correspondence of the $CFCl_3$ band at 846 cm^{-1} and the CF_2Cl_2 band at 923 cm^{-1} are attributable to differences in the amounts used in kCARTA and LBLRTM whereas residuals around 880 cm^{-1} should be attributed to the spectroscopy. In the window region between 1080 and 1200 cm^{-1} the change in the continuum reduces the peak-to-peak differences and shifts the biases towards positive values. This would suggest that in this spectral region differences between the spectra are attributable primarily to differences between the molecular databases.

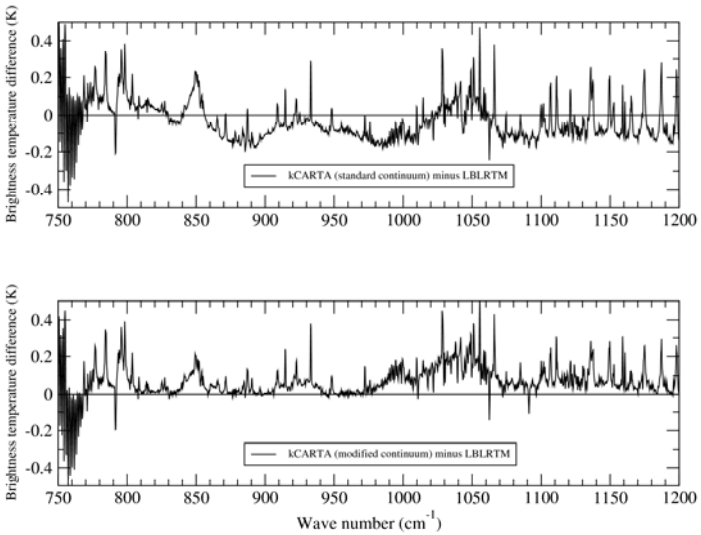

Figure 5: The difference between a) kCARTA and LBLRTM in the tropical region; b) kCARTA_LBL and LBLRTM in the tropical region.

3.2. IASI band 2 (1200 to 2000 cm^{-1})

Results for IASI band 2 in the northern hemisphere are shown in Fig. 6. Biases vary between -0.8 and 0.8K although larger values up to -1.4K are observed for channels located in the spectral region characterized by the presence of the strong ν4-band of methane at 1310 cm^{-1}. The same spectral region is characterized by large negative biases. This can be partly explained by the fact that methane amounts are fixed to climatological values.

LBLRTM and kCARTA spectra exhibit very similar features in the left side and central part of the water vapour ν2 band from 1400 up to 1700 cm^{-1}. In this spectral region the GENLN2 spectrum is more irregular and probably reflects differences in the spectroscopy. This is all the more evident around 1600 cm^{-1} where GENLN2 shows significantly larger biases. We attribute this feature to the water vapour continuum model that in the case of GENLN2 uses smaller values of the spectral density function in this region.

To the right side of the band, the structure of the spectra is more irregular. The GENLN spectrum follows more closely the LBLRTM spectrum and in the case of kCARTA we can observe a consistent number of spikes that are not present in spectra obtained using the other LBL models.

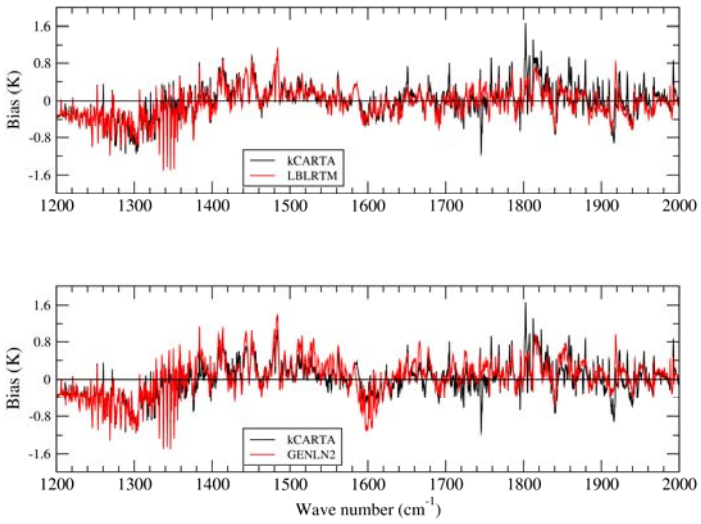

Figure 6: The mean value of the difference between observed and computed brightness temperatures in the northern hemisphere for IASI band 2.

Results for the tropical region are shown in Fig. 7. All the spectra are characterized by larger biases that, with the exception of channels in the methane band where values can reach -2K, vary between -0.8 and 1K. In contrast to what observed in the northern hemisphere, biases in most of the spectral regions are offset toward positive values. This might reflect the presence of wet biases in the ECMWF humidity fields. Differences between the spectra are now larger and the structure of the spectra is more articulate. It would appear that in general LBLRTM tends to fit better the observations although it is difficult to give a conclusive answer since the results can be affected by uncertainties in the water vapour profiles above all in presence of the high water vapour loadings characteristic of tropical conditions.

In terms of absolute biases, results obtained in the southern hemisphere (shown in Fig. 8) are comparable to those obtained in the northern hemisphere with the exception of the region between 1980 and 2000 cm^{-1} where the LBLRTM spectrum exhibits larger biases.

Since GENLN2 and kCARTA use the same molecular database it is difficult to explain the origin of the large spikes in the kCARTA spectra since these cannot attributed to the continuum model. In fact the experiment described in section 3.1.3 where kCARTA spectra have been computed using the same water vapour continuum model used in LBLRTM shows that differences between the kCARTA and LBLRTM continuum can only have a significant impact in the spectral regions at the edges of the band. Hence, the vast majority of the spikes seen in kCARTA cannot be attributed to the continuum model. This is also true for the other geographical regions. The same experiment shows that in the tropics and in the southern hemisphere, differences between kCARTA and LBLRTM in the region between 1970 and 1990 cm^{-1} and between 1200 and 1280 cm^{-1} are almost entirely attributable to the continuum model.

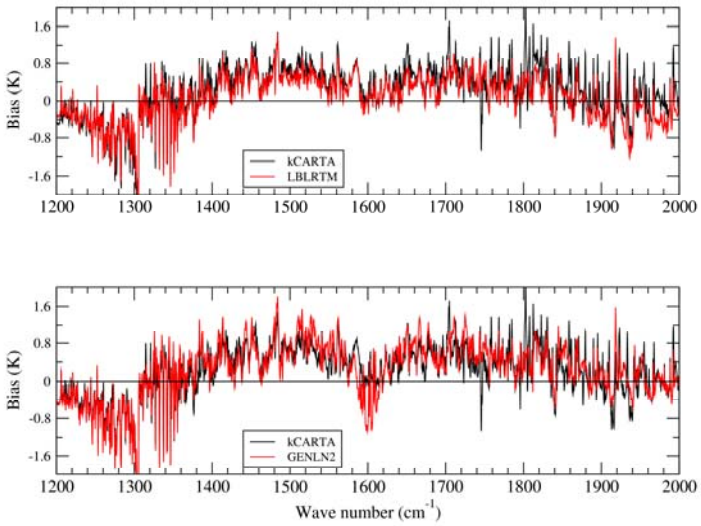

Figure 7: The mean value of the difference between observed and computed brightness temperatures in the tropical region for IASI band 2.

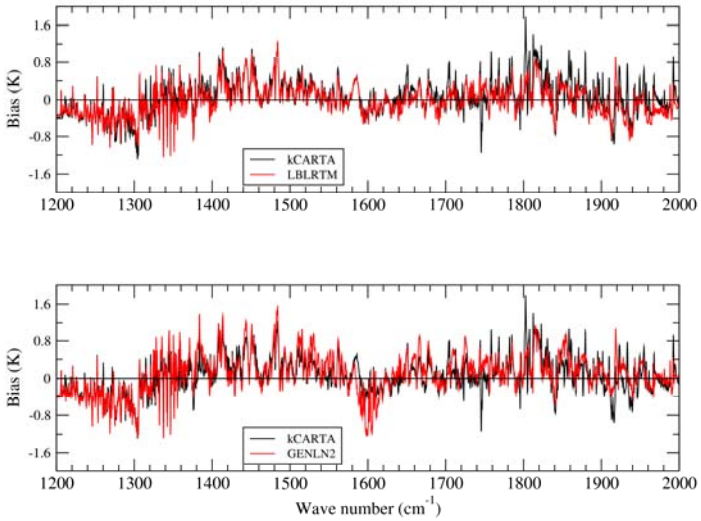

Figure 8: The mean value of the difference between observed and computed brightness temperatures in the southern hemisphere for IASI band 2.

3.3. IASI band 3 (2000 to 2760 cm^{-1})

Results for IASI band 3 are shown in Fig. 9, Fig. 10 and Fig. 11 for the northern hemisphere, tropics and southern hemisphere respectively. Larger biases between 2080 and 2200 cm^{-1} in the southern hemisphere and in the tropics reflect large latitudinal gradients of CO amounts not accounted for in the RT computations. In the same spectral region biases in the northern hemisphere vary between -0.4K and 0.4K reflecting smaller CO latitudinal gradients. Large spikes in the kCARTA spectra are still present and are a noticeable feature between 2000 and 2150 cm^{-1}.

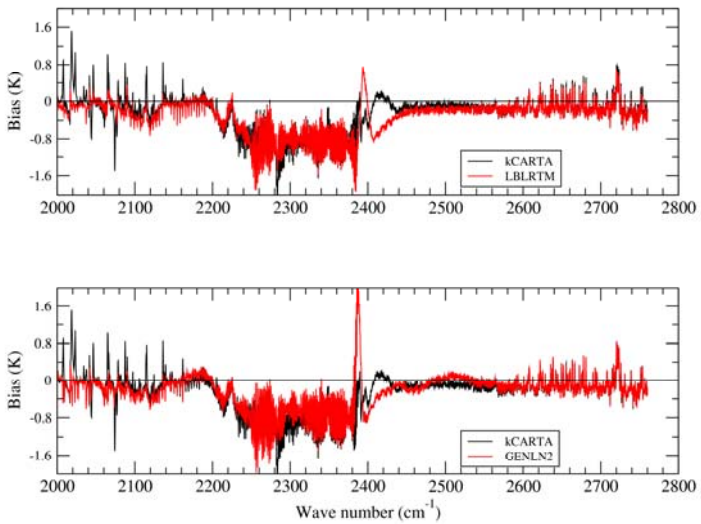

Figure 9: The mean value of the difference between observed and computed brightness temperatures in the northern hemisphere for IASI band 3.

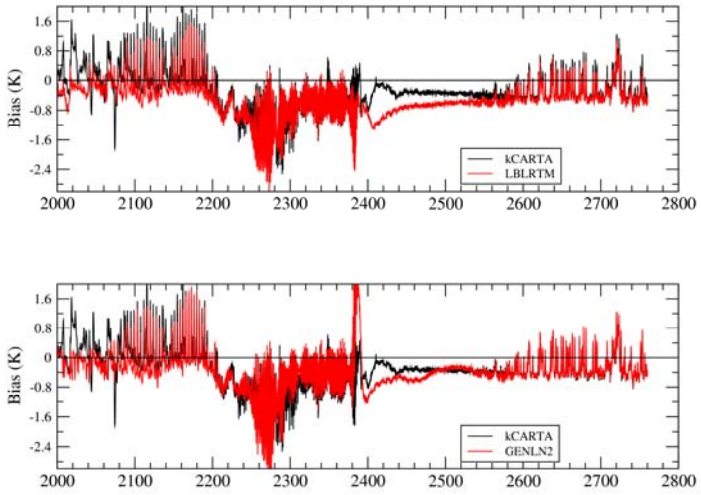

Figure 10: The mean value of the difference between observed and computed brightness temperatures in the tropics for IASI band 3.

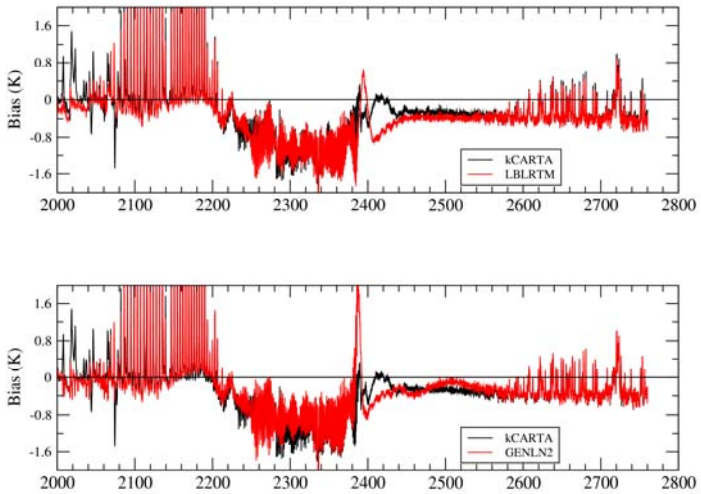

Figure 11: The mean value of the difference between observed and computed brightness temperatures in the southern hemisphere for IASI band 3.

3.3.1. Results in the temperature sounding band

The biases observed in the υ3-CO_2 band are larger than biases in the υ2- band. The spectral region between 2200 and 2300 cm^{-1} is characterized by the presence of tropospheric temperature sounding channels. The inconsistency between tropospheric temperature sounding channel biases in the long-wave and short-wave region points to larger errors in the short-wave CO_2 line parameters. The region between 2300 and 2380 cm^{-1} sees the presence of a large number of channels characterized by very high-peaking weighting functions with tails that can extend well into 0.2 hPa. Consequently, the large biases observed in this region might be associated to biases in the ECMWF stratospheric and mesospheric temperature profiles.

Between 2200 and 2380 cm^{-1} biases in the northern and southern hemisphere assume negative values that vary between -1.8K and -0.4K. LBLRTM and GENLN exhibit larger biases around 2260 cm^{-1} whereas kCARTA exhibits larger biases around 2280 cm^{-1}. Biases between 2320 and 2380 cm^{-1} are very similar. In the tropical region we observe the same pattern. However, biases between 2320 and 2380 cm^{-1} are now smaller whereas biases around 2280 cm^{-1} are much larger with GENLN2 attaining values as large as -3K. We tend to interpret the close similarities between the GENLN2 and LBLRTM spectra in terms of the line mixing model.

As shown in our plots, GENLN2 spectra in the region between 2380 and 2400 cm^{-1} exhibit biases that are typically larger than biases in the equivalent kCARTA and LBLRTM spectra. In this region P/R-branch line mixing plays a major role and we tend interpret this result as a consequence of errors in the GENLN2 Cousin CO_2 line shape. It should be noted that as a result of the symmetry of the states involved in the molecular transitions, P/R-branch line mixing is expected to be twice as strong than in the υ2-band. If the behaviour of GENLN2 is justified on the grounds of inaccurate line shape, the LBLRTM spectra show that there are still issues with the modelling of CO_2 line shape in the CO_2 υ3-bandhead. This is also true, albeit to a much lesser extent, for kCARTA. In particular, between 2380 and 2400 cm^{-1} the LBLRTM spectra show large oscillations whose amplitude can reach almost 3K in the northern hemisphere. It is possible that this result could be associated to biases in the ECMWF temperature profiles but we would like to bring forward the hypothesis that this behaviour might in fact be related to the treatment of the CO_2 continuum in LBLRTM. Our spectra could indicate that the scaling factor of 0.75 applied to the CO_2 continuum might not be universally valid.

3.3.2. Results in the window region

Biases in the 2500 cm^{-1} window region are influenced by the same factors discussed in section 3.1.3. Like in band 1, spectra in the northern and southern hemispheres are closer than spectra in the tropics. However, opposite to what observed in band 1, biases in the southern hemisphere tend to be larger than biases in the northern hemisphere. Biases are generally negative but a small number of positive values are also observed. In terms of absolute values, biases vary between -0.4 and 0.8 K.

Differences between the spectra largely reflect differences between the continua models. The change in the kCARTA continuum model has an impact between 2380 and 2660 cm^{-1}. The use of the same LBLRTM water continuum model reduces to naught differences between kCARTA and LBLRTM in the 2440 to 2624 cm^{-1} spectral region. Hence, in this spectral region differences between kCARTA and LBLRTM can be attributed solely to the water continuum whereas between 2400 and 2440 cm^{-1} the origin of the differences between the LBLRTM and kCARTA is not in the water continuum. In fact, as suggested in the previous section, it might be related to the LBLRTM CO_2 line shape. It would also appear that the kCARTA spectra are in better agreement with observation suggesting that the modifications made to the continuum model have improved the accuracy of the spectra.

Beyond 2624 cm^{-1}, differences between the spectra are attributable to the water vapour spectroscopy. This is clearly demonstrated by the fact the kCARTA spectra are in better agreement with the GENLN2 spectra (the two models use the same molecular database). In this region dominated by line absorption, results tend to suggest that the spectroscopic parameters used in LBLRTM fit marginally better the observations.

4. Conclusions

Four monitoring experiments have been carried out to compare IASI observed radiances to radiances simulated by the RTTOV fast radiative transfer model using regression coefficients based on the GENLN2, kCARTA and LBLRTM LBL models using different molecular databases. Results obtained from IASI data between the 1st April 2008 and the 15th April 2008 using clear channels (i.e. channels not affected by clouds) over the sea show that in the northern and southern hemisphere biases in IASI band 1 and 2 are typically within ±1K. In the tropics, biases in the water vapour ν2- band do increase but for most of the channels the peak-to-peak value is still within within ±1K. The larger biases observed in the water vapour band tend to reflect errors in line parameters generated by spectroscopic errors and by the inaccurate specification of the water vapour profiles. Spectra obtained in the tropics in fact suggest the presence of a wet bias in the ECMWF humidity fields. The use of the MT_CKD continuum model results in a reduction up to 1K of the biases in the region around 1600 cm^{-1}. The large biases observed in the ozone band in the northern hemisphere probably reflect a poorer performance of the ozone assimilation system in this geographical region. A more accurate description of the CO_2 line shape has a significant impact on the simulated radiances in the CO_2 ν2-band resulting in a reduction of the biases up to 1K. In the same band large biases are observed in the centre of the Q-branch at 667 cm^{-1}. In the important temperature sounding CO_2 ν3-band we obtained biases significantly larger than biases observed in the ν2-band and we tend to attribute this result to larger spectroscopic errors and to biases in the ECMWF temperature profiles. The kCARTA and LBLRTM improvements in the CO_2 line shape result in smaller biases in the CO2 ν3-bandhead. However, the LBLRTM spectra display large oscillations not seen in the kCARTA spectra. We have tentatively suggested that this behaviour is related to the LBLRTM CO_2 line shape, in particular the model used for the CO_2 continuum.

Acknowledgements

We want to thank P. Brunel (Météo France) for having made available the kCARTA coefficients, C. Clerbaux (Service d'Aéronomie) for having made available concentrations for minor gas species, T. McNally (ECMWF) for the very helpful collaboration received during the set up of the monitoring experiments and A. Collard (ECMWF) and N. Bormann (ECMWF) for the implementation of IASI and RTTOV-9 in the ECMWF data assimilation system.

References

Clough, S.A., Kneizys, F.X., and Davis R.W.: Line shape and the water vapour continuum, Atmospheric Research, 23, 229-241, 1989.

Clough, S.A, Iacono, M.J. and Moncet J.-L.: Line by line calculation of atmospheric fluxes and cooling rates: application to water vapor, J. Geophys. Res., 98, pp. 15761-15785, 1992.

Collard, A.D., and McNally, A.P.:Assimilation of IASI radiances at ECMWF, Q. J. Roy. Meteorol. Soc., in review, 2008.

Cousin, C., Le Doucen, R., Boulet, C., and Henry, H.: Temperature dependence of the absorption in the region beyond the 4.3 μm band head of CO2. Part 2: N2 and O2 broadening, Applied Optics, 24, 3899-3907, 1985.

De Souza-Machado, Strow, L.L., Tobin, D., Motteler, H., and Hannon, S.E.: Improved atmospheric radiance calculations using CO2 p/r-branch line mixing, in Proc. Euro. Symp. Aerospace Remote Sensing Europto Series, 1996.

De Souza-Machado, Strow, L.L., Motteler, H., and Hannon, S.E.: kCARTA: an atmospheric radiative transfer algorithm using compressed lookup tables. Univ. Maryland Baltimore County, Dept. Physics, Tech. Report, available at http://asl.umbc.edu/pub/rta/kcarta, 2002.

De Souza-Machado, S.:Personal comunication, 2008.

Edwards, D.P.: GENLN2. A general Line-by-Line Atmospheric Transmittance and Radiance Model, NCAR Technical note NCAR/TN-367+STR, National Center for Atmospheric Research, Boulder,Co, 1992.

Hauglustaine, D.A., G.P. Brasseur, S. Walters, P.J. Rasch, J.-F. Müller, L.K. Emmons, and M.A. Carroll, MOZART, a global chemical transport model for ozone and related chemical tracers, 2, Model results and evaluation, J. Geophys. Res., 103, 28,291-28,335, 1998.

Jacquinet-Husson, N., Scott, N.A., Chedin, A., Garceran, K., Armante,R., Chursin, A.A.,Barbe, A., Birk, M., Brown, L.R., Camy-Peyret, C., Claveau, C.,Clerbaux, C., Coheur, P.F., Dana, V., Daumont, L.,Debacker-Barilly, M.R.,Flaud, J.M.,Goldman, A.,Hamdouni, A.,Hess, M.,Jacquemart, D., Kopke, P., Mandin, J.Y., Massie, S., Mikhailenko, S., Nemtchinov, V., Nikitin, A., Newnham, D., Perrin, A., Perevalov, V.I., Regalia-Jarlot, L., Rublev, A., Schreier, F., Schult, I., Smith, K.M., Tashkun, S.A., Teffo, J.L., Toth, R.A., Tyuterev, Vl. G.,Vander Auwera, Varanasi, J.P., Wagner, G.: The 2003 edition of the GEISA/IASI spectroscopic database, J. Quant. Spectrosc. Radiat. Transfer, 95, 429-467, 2005.

Masiello, G., Serio, C., Carissimo, A., Grieco, G., and Matricardi, M.:Application of φ-IASI to IASI: retrieval products evaluation and radiative transfer consistency, Atmos. Chem. Phys., in review, 2009.

Matricardi, M.: RTIASI-4, a new version of the ECMWF fast radiative transfer model for the infrared atmospheric sounding interferometer, ECMWF Research Dept. Tech. Memo. 345, http://www.ecmwf.int/publications, 2003.

Matricardi, M., Chevallier, F., Kelly, G., and Thepaut, J.-N.: An improved general fast radiative transfer model for the assimilation of radiance observations, Q. J. Roy. Meteorol. Soc., 130, 153-173, 2004.

Matricardi, M.: An inter-comparison of line-by-line radiative transfer models, ECMWF Research Dept. Tech. Memo. 525, http://www.ecmwf.int/publications, 2007.

Matricardi, M.: The generation of RTTOV regression coefficients for IASI and AIRS using a new profile training set and a new line-by-line database, ECMWF Research Dept. Tech. Memo. 564, http://www.ecmwf.int/publications, 2008.

McNally, A.P. and Watts, P.D.: A cloud detection algorithm for high-spectral-resolution infrared sounders, Q J Roy Meteorol Soc, 129, 3411-3423, 2003.

Niro, F., Jucks, K., and Hartmann, J.-M.: Spectra calculations in central and wing regions of CO2 IR bands. IV: software and database for the computation of atmospheric spectra, Journal of Quantitative Spectroscopy and Radiative Transfer, Volume 95, Issue 4, 469-481, 2005.

Rizzi, R., Matricardi, M., and Miskolczi, F.: Simulation of Uplooking and Downlooking High-Resolution Radiance Spectra With Two Different Radiative Transfer models, Appl. Opt. 41, 940-956, 2002.

Rothman, L.S., Barbe, A., Chris Benner, D., Brown, L.R., Camy-Peyret, C., Carleer, M.R., Chance, K., Clerbaux, C., Dana, V., Devi, V.M., Fayt, A., Flaud, J.-M., Gamache, R.R., Goldman, A., Jacquemart, D., Jucks, K.W., Lafferty, W.J., Mandin, J.-Y., Massie, S.T., Nemtchinov, V., Newnham, D.A., Perrin, A., Rinsland, C.P., Schroeder, J., Smith, K.M., Smith, M.A.H., Tang, K., Toth, R.A., Vander Auwera , J., Varanasi, P., Yoshino, K.: The HITRAN molecular spectroscopic database: edition of 2000 including updates through 2001, J. Quant. Spectrosc. Radiat. Transfer, 82, 5-44, 2003.

Rothman, L.S., Jacquemart, D., Barbe, A., Chris Benner, D., Birk, M., Brown, L.R., Carleer, M.R., Chackerian Jr., Chance, C.K., Coudert, L.H., Dana, V., Devi, V.M., Flaud, J.M., Gamache, R.R., Goldman, A., Hartmann, J.M., Jucks, K.W., Maki, A.G., Mandin, J.Y., Massie, S.T., Orphal, J., Perrin, A., Rinsland, C.P., Smith, M.A.H., Tennyson, J., Tolchenov, R.N., Toth, R.A., Vander Auwera, J., Varanasi, P., Wagner, G.: The HITRAN 2004 molecular spectroscopic database, J. Quant. Spectrosc. Radiat. Transfer, 96, pp.139-204, 2005.

Saunders, R., Matricardi, M. and Brunel, P.: An improved fast radiative transfer model forassimilation of satellite radiance observations, Quart. J. Roy. Meteor. Soc., 144, 1547-1558, 1999.

Saunders, R., Matricardi, M., and Geer, A.: Rttov9.1 users guide, NWP SAF report, Met. Office, 57pp., 2008.

Strow, L.L., Tobin, D.C., and Hannon, S.E.: A compilation of First-Order Line-Mixing coefficients for CO2 Q-branches. J. Quant. Spectrosc. Radiat. Transfer, 52, 281, 1994.

Strow, L. L., Motteler, H.E., Benson, R.G., Hannon, S.E., and De Souza-Machado, S.: Fast computation of monochromatic infrared atmospheric transmittances using compressed lookup tables, J. Quant. Spectrosc. Radiat. Transfer, 59, 481-493, 1998.

Strow, L.L., Hannon, S.E., De Souza-Machado, Motteler, S.H., and Tobin, D.: An Overview of the AIRS Radiative Transfer Model, IEEE Transactions on GeoSciences and Remote Sensing, 41, 274, 2003.

Tjemkes, S.A., Patterson, T., Rizzi, R., Shephard, M.W., Clough, S.A., Matricardi, M., Haigh, J.D., Höpfner, M., Payan, S., Trotsenko, A., Scott, N. Rayer, P., Taylor, J.P., Clerbaux, C., Strow, L.L., DeSouza-Machado, S., Tobin, D., and Knuteson, R.: The ISSWG line-by-line inter-comparison experiment, J. Quant. Spectrosc. Radiat. Transfer, 77, 433-453, 2003.

Tobin, D.C.: Infrared spectral lineshapes of water vapour and carbon dioxide, Ph.D. dissertation, Univ. Maryland Baltimore County, Baltimore, MD, 1996.

Tobin, D.C., Best, F.A., Brown, P.D., Clough, S.A., Dedecker, R.G., Ellingson, R.G., Garcia, R.K., Howell, H.B., Knuteson, R.O., Mlawer, E.J., Revercomb, H.E., Short, J.F., van Delst, P.F.W., and Walden, V.P.: Downwelling spectral radiance observations at the SHEBA ice station: Water vapor continuum measurements from 17 to 26 μm, J. Geophys. Res., 04/D2, 2081-2092, 1999.